

ABSTRACT

Our goal is to use thermal imaging to diagnose a particle accelerator used in medicine. This technic can track its operating status and detect breakdowns and failures. The accelerator is used in the Regional Cancer Center in Oujda (CRO) to treat cancerous patients. The CRO plays a crucial role in the medical area of eastern morocco. Hence, to better manage and plan the therapeutic sessions, we have to ensure an upstream apparatus diagnosis. Our work involves the production of a thermal mapping of the accelerator during normal operating and when a failure occurs. The analysis begins with the manual segmentation of thermal images to isolate different significant regions. Afterwards, we will determine the temperature of all interesting present elements in the area. Finally, we will conduct a comparison of accelerator components temperature in the case of normal operating and when is down. Therefore, the analysis of the thermal mapping will help us identify the defective element and prevent any further deterioration.

KEYWORDS: Radiation, infrared thermography, diagnosis, maintenance, temperature, measurements.

INTRODUCTION

With Planck's law [8], it is possible to obtain the temperature of any object accurately, which allows us judging very quickly the behavior of the apparatus. Indeed, the material permanently exchanges energy with the external environment in the form of electromagnetic radiation. In this manner, any material of which the temperature is above 0°K, radiates heat in the infrared spectrum. Recently, the infrared thermography is intensively explored in

machine diagnosis [1-7]. This technique is based on radiative heat flux measurement without contact with the subject [9]. At the time being, almost all devices heat before breaking down. This temperature fluctuation may be due to various reasons such as contact problems, current overload, overvoltage or cracks in the insulation, which could result in unplanned outages. Therefore, the preventive diagnosis of possible thermal anomalies is required. This work deals with the application of this non-destructive technique and not offensive to make the particle accelerator diagnosis and follow his condition. Our analysis is built upon the segmentation of the thermal image in order to isolate the significant regions and to determine the temperature of the important areas. This technique will not only detect the problem, but it could also impede the influence on the other components.

MATERIALS AND METHODS

Theoretical basis of infrared detector

The infrared camera used in this work is “Flir-440” (www.flir.com). The instrument is able of measuring the surface temperature with a precision of 0.1°C, which can produce thermograms that represent the surface temperatures. The principle of an infrared camera operating is based on the following process: The heat emitted in the form of infrared radiation is received by an infrared sensor. The latter converts the collected thermal energy into electrical signals which are then displayed in terms of temperature by a suitable electronic system. In this way, the thermal imaging transforms infrared radiation measures into thermogram. Each image pixel corresponds to a given color and a specific temperature.

The infrared radiation theory is based on the black body described by Planck in [8]. The latter is able to absorb any incident radiation regardless of its wavelength and emit in turn radiation of all wavelengths. The radiation of a black body is defined by the three following laws.

Planck’s law

This law gives the spectral energy radiated by a black body as a function of wavelength and temperature [10]. It is given by the following equation eq. (1)

$$I_o(\lambda, T) = \frac{2hc^2}{\lambda^5} \frac{1}{e^{\frac{hc}{\lambda kT}} - 1} \quad (1)$$

- with
- c : the speed of light (m/s)
 - h : Planck’s constant (J.S)
 - k_b : Boltzmann’s constant (J /°K.)
 - λ : wavelength (m)
 - T : absolute surface temperature of the blackbody (°K)

The graphical representation of Planck’s law (Figure.1) shows that at large wavelengths, the radiated power for a given temperature is not at its maximum value. Thus, it is extremely difficult to detect the flux emitted by a body and subtract to ambient electrical and thermal noise. In our case, the accelerator, ELEKTA emits radiation in the range $[\lambda_{max}^1 = 8.78 \mu m ; \lambda_{max}^2 = 10.35 \mu m]$ which corresponds to the temperature range $[T_1 = 280^\circ K ; T_2 = 330^\circ K]$

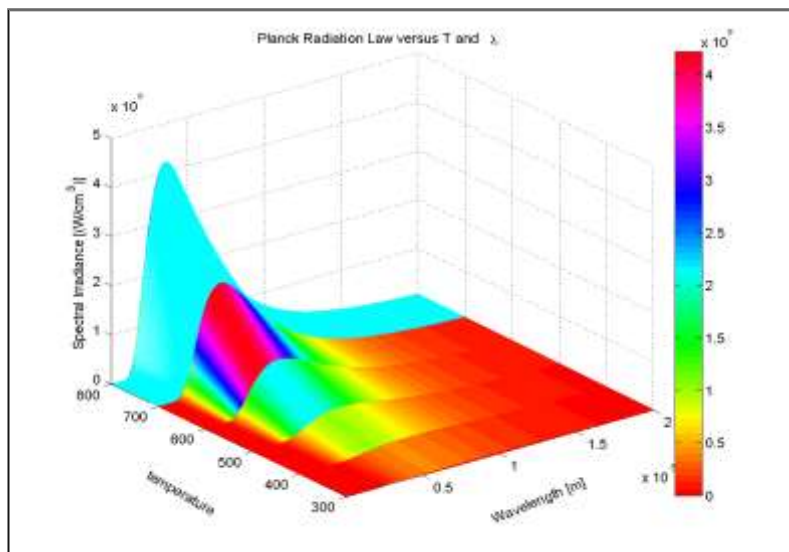


Figure 1: Radiation versus λ for different temperature values.

Wein's law

The wavelength at which the Planck distribution reaches the maximum specific value is marked by a dotted line from the maxima of the curves (Figure.2) and is given by the Wien's displacement law. Eq. (2). It expresses that the color of a heated object at an elevated temperature varies from red to with:

$$\lambda_{\max} = \frac{2898}{T} \quad (2)$$

This law suggests that the hotter a body is, the shorter wavelengths are radiated. For example the apparent temperature of the sun is 6000 °K, which shines around 0.5µm. The accelerator, by which our measurements were made, reaches a temperature of about 333 °K which corresponds to a maximum emittance around 9 µm.

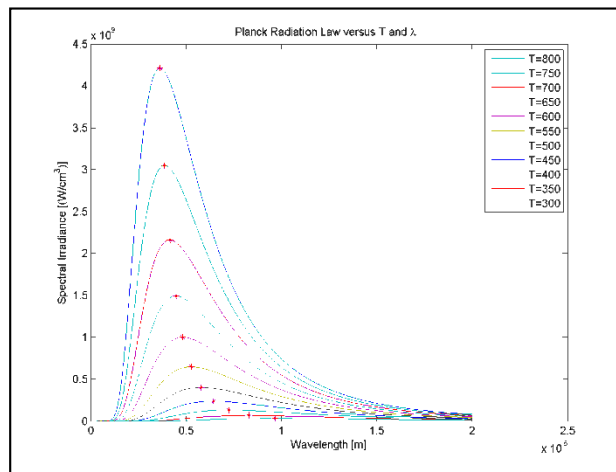


Figure 2: Wein's law.

The Stefan-Boltzmann law

It shows that the total radiant emittance integrated over all wavelengths, is proportional to the fourth power of its absolute temperature see (Figure.3). It is given by eq. (3):

$$I_0(T) = \sigma T^4 \quad (3)$$

With : $\sigma = 5,67.10^{-12} \text{ Wcm}^{-2}\text{K}^{-4}$

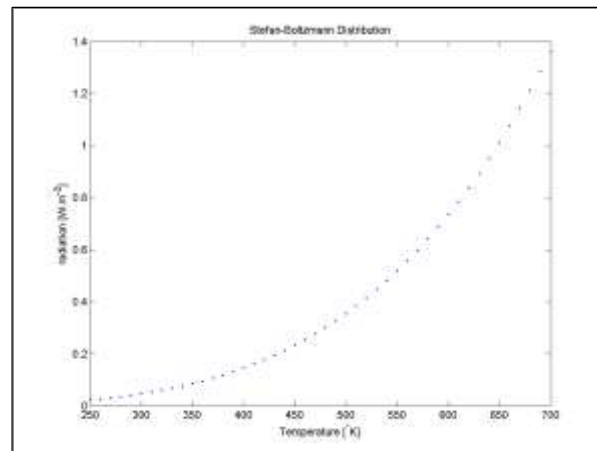


Figure 3: Stefan-Boltzman's law.

Emissivity

The emissivity is a thermal radiation report from a real surface at a given temperature to that of a black body under the same conditions (temperature, wavelength and direction).

The emissivity coefficient is a number value between zero and one. It corresponds to the amount of heat that can be absorbed by the surface. A value close to the maximum absorbs heat well, while a value close to zero almost completely reflects heat. This coefficient that is given by eq. (4):

$$\varepsilon = \frac{I(\lambda, T)}{I_0(\lambda, T)} \quad (4)$$

With :

- $I(\lambda, T)$: Energy radiated from a real body
- $I_0(\lambda, T)$: Energy radiated by a blackbody

RESULTS AND DISCUSSION

Infrared radiation is invisible to naked eye. Therefore, the radiated energy in the infrared band is to be transformed into a visible image through appropriate equipment [12]. Indeed our measurements are taken with a Flir-440 (www.flir.com) infrared camera. This method is requested because of its non-intrusive and non-destructive nature. Our task is to identify the breakdown of component in case of failure in the accelerator. Likewise, it helps to monitor its status and determine the temperature of each component in real time. This controls the device and tracks the spread of the breakdown in the components. In this section, we present measurements on the CRO accelerator. These measurements were taken during normal operating and during the presence of a breakdown. The interpretation of thermal maps obtained based on the manual segmentation of images and the determination of the temperature of all elements present in a specific band.

Area segmentation and interpretation

The segmentation of an image is the process of partitioning the corresponding graph into several significant areas. It can be automated by using the segmentation technique [11]. Such technique detects the location defining edges when significant variation of a grayscale; or grayscale thresholding aims to segment an image into several classes using only its histogram. It is, therefore, assumed that only the information associated with the image allows segmentation. Therefore, segmentation allows identifying different objects that constitute the scene of the picture that is, sometimes, invisible to naked eye before image treatment. However, we can manually separate areas of interest when they are easily highlighted. In our case, the thermal mapping clearly shows several important regions on the surface of the accelerator (Figure.4).

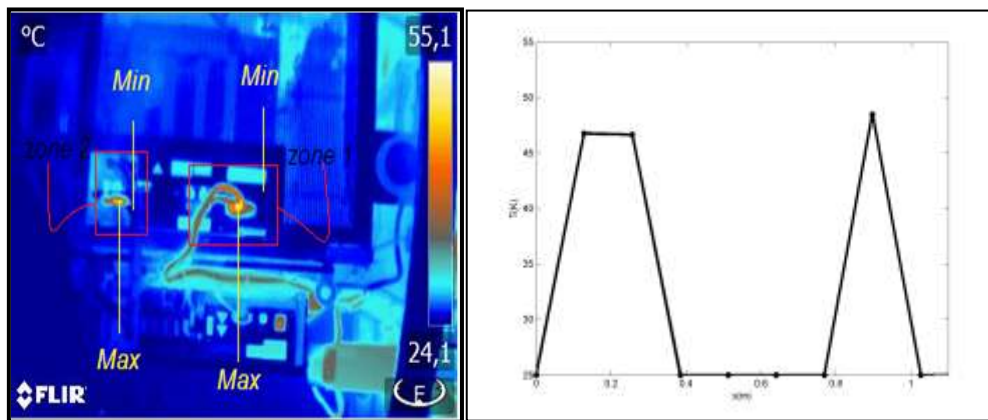


Figure 4: Accelerator thermogram in normal operating and the components temperature versus their positions.

Expressive area treatment

After specifying the area to be treated in the thermal image, we determine the relationship between color and temperature by exploiting the color scale. Indeed, the color-temperature assignment consists of a palette treatment, that is, screening object temperature by its color. Our color scale reads a temperature range [24.1 °K; 55.1 °K] corresponding to a color range from blue to white (Figure.4).

We use these data to ascertain the temperature of each pixel from the color triplet (RGB). Afterwards, we reveal the temperature of different zones indicated on the (Figure.4). The use of the MatLab software enables us to realize the temperature of each pixel in the image. Therefore, we plot temperature depending on the accelerator component positions (Figure.4).

We repeated the measurement in the same conditions when the accelerator is down. Thermal mapping of the accelerator obtained is given in (Figure.5).

The analysis of the image allows setting the temperature of the strip containing the two known areas depending on their position.

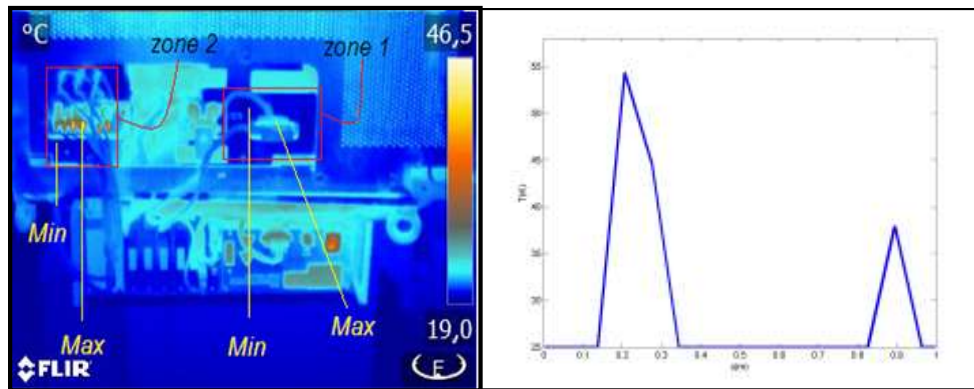


Figure 5: Accelerator thermogram when is down and the components temperature versus their positions.

The temperature curves comparison shows a significant difference between the temperatures (figure.6) of a component located in the region between 15cm and 35cm. This directs us to the breakdown site. Furthermore, the sensitive elements could be monitored by the band temperature reading.

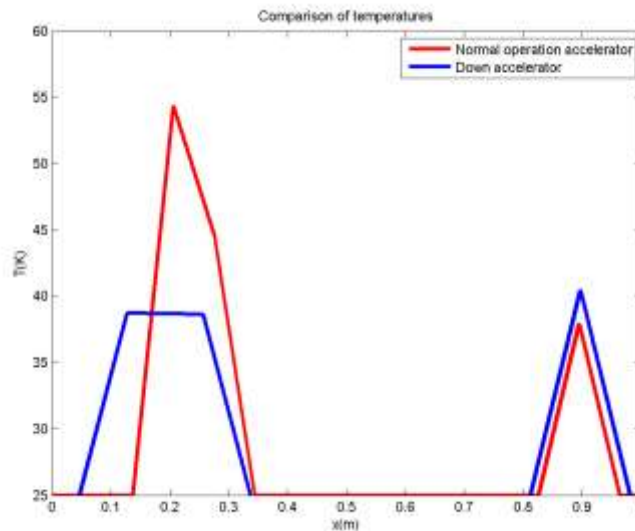


Figure 6: Temperature of accelerator in normal operating and when it was down.

CONCLUSION

Currently infrared thermography is used in a broad spectrum. We applied this technique on a particle accelerator used in medical purposes. In this manner, we present the results of its thermography. We perform a thermal mapping of the apparatus during its normal operating and when a failure occurred. Our analysis leads us to find out the defect. The technique can also tracks down the spread of the failure and reveals the degradation of the components, which will hinder the propagation of the blemish to other accelerator components. Therefore, we can establish an optimum session therapeutic planning and take an appropriate decision before failure occurs.

ACKNOWLEDGEMENTS

We seize this opportunity to express our gratitude and warmth thanks to the directors of the CHU, the CRO and the technological platform of Industrial Engineering of the ENSAO for their technical and logistical support.

REFERENCES

- [1] Angeliki Kylili, Paris A. Fokaides, Petros Christou, Soteris A. Kalogirou, Infrared thermography (IRT) applications for building diagnostics: A review. *Applied Energy* 134 (2014) 531–549.
- [2] Oliver Faust, U. Rajendra Acharya, E.Y.K. Ng, Tan Jen Hong, Wenwei Yu, Application of infrared thermography in computer aided diagnosis. *Infrared Physics & Technology* 66 (2014) 160–175.
- [3] A.S. Nazmul Huda, Soib Taib, Application of infrared thermography for Predictive/preventive maintenance of thermal defect in electrical equipment, *Applied Thermal Engineering* 61, pp. 220-227, 2013.
- [4] Mohd Shawal Jadin, Soib Taib, Recent progress in diagnosing the reliability of electrical equipment by using infrared thermography, *Infrared Physics & Technology*, 55 (2012), pp. 236–245.
- [5] Armando Guadalupe Garcia-Ramirez, Luis Alberto Morales-Hernandez, Roque Alfredo Osornio-Rios, Juan Primo Benitez-Rangel, Arturo Garcia-Perez, Rene de Jesus Romero-Troncoso, Fault detection in induction motors and the impact on the kinematic chain through thermographic analysis, *Electric Power Systems Research* 114 (2014), pp. 1–9.
- [6] F. Jeffali, B. EL Kihel, A. Nougouai & F. Delaunois. Monitoring and diagnostic misalignment of asynchronous machines by Infrared Thermography, *J. Mater. Environ. Sci.* Vol. 6, N0 4, pp. 1192-1199, 2015
- [7] Abbas K. Abbas, Konrad Heimann, Vladimir Blazek, Thosten Orlikowsky, Steffen Leonhardt, Neonatal infrared thermography imaging: Analysis of heat flux during different clinical scenarios, *Infrared Physics & Technology* 55(2012), pp. 538-548.
- [8] Max Planck, On the Law of Distribution of Energy in the Normal Spectrum, *Annalen der Physik*, vol. 4, p. 553 ff (1901).
- [9] D. Pajani, Thermographie - Principes et mesure, *Technic de l'Ingénieur*, r2740 (2013).
- [10] Clayton A. Gearhart, Planck, the Quantum, and the Historians, *Phys. perspect.* 4 (2002) 1, 1422–6944/02/040170–461.\$50+0.20/0.
- [11] Chin-Ya Huang, Mon-Ju Wu ECE 533 Final Project, Fall 2006 University of Wisconsin- Madison.
- [12] G. gaussorges, *La thermographie infrarouge*, première édition, 1981.